

A 1.3-Myr palaeoceanographic record from the continental margin off Dronning Maud Land, Antarctica

Carl Fredrik Forsberg^a, Reidar Løvlie^b, Eystein Jansen^c, Anders Solheim^a, Hans Petter Sejrup^c and Hans Erik Lie^d

^a Norwegian Geotechnical Institute, P.O. Box 3930, Ullevål Hageby, N-0806, Oslo, Norway

^b Department of Solid Earth Physics, University of Bergen, Allégt 41, N-5007, Bergen, Norway

^c Department of Geology, University of Bergen, Allégt 41, N-5007, Bergen, Norway

^d Norsk Hydro A/S, Sandvika, Norway

Received 22 April 2002; accepted 3 March 2003. ; Available online 26 August 2003.

Abstract

A 12.5 m long core was retrieved from the continental margin off Dronning Maud Land, Antarctica. Magnetostratigraphy, stable isotopes, ¹⁴C accelerator mass spectrometer and amino acid analyses indicate a continuous sediment record going back 1.3 Myr. Comparison of CaCO₃ results with those from ODP

Site 1089 and an index of North Atlantic Deep Water (NADW) influence in surface waters indicate that NADW upwelled along the Antarctic continental margin during the whole of this period. The mid-Pleistocene transition (1.0–0.6 Ma) was accompanied by an apparent decline in the NADW influence, and was followed by extended carbonate dissolution during the interglacials of marine isotope stages (MIS) 13 and 11. Less extensive periods of dissolution occur at the end of the interglacials younger than MIS 11. While interglacial dissolution is characteristic of the Pacific and Indian oceans, the carbon isotopes return to pre-transition values indicative of renewed NADW upwelling. The concentration of ice-rafted debris may reflect changes in the relative rate of interglacial sedimentation. It is speculated that the high ice rafted debris (IRD) concentrations during interglacials younger than 400 kyr may be due to a reduced relative sedimentation rate of other interglacial components whereas the low concentrations during interglacials before the mid-Pleistocene transition may be due to a higher relative sedimentation rate of these.

Author Keywords: Antarctic; Weddell Sea; Dronning Maud Land; palaeoceanography; stable isotopes; magnetostratigraphy

1. Introduction

The Southern Ocean is both a mixing ground for the world's water masses and a region containing steep latitudinal and vertical oceanographic gradients. North Atlantic Deep Water (NADW) mixes with Antarctic Circumpolar Water (ACW) in the Atlantic sector of the Southern Ocean and wells up south of the Antarctic Polar Front (APF, [Fig. 1b](#)), along the Antarctic continental margin. While there are indications that millennial-scale climatic changes in the two hemispheres may be out of phase (e.g. [\[Broecker, 1998\]](#)), there are also indications that changes in the intensity of NADW circulation at Milankovitch periods is reflected in the carbon isotopic composition of ACW ([\[Oppo et al., 1995\]](#)). We will here concentrate on the Milankovitch-scale changes in ocean circulation and on the NADW contribution to the palaeoceanography of the Antarctic continental margin. However, very few long records (e.g. [\[Bonn et al., 1998\]](#), [\[Pudsey, 1992\]](#) and [\[Mackensen et](#)

al., 1989)) have been published from the continental slope of the Atlantic sector of Antarctica. Of these, only one record, to the author's knowledge, ([Mackensen et al., 1989]) extended back past the Brunhes–Matuyama geomagnetic reversal, but this record exhibited an apparently disturbed interval between marine isotope stages (MIS) 13 and 9 that made it difficult to interpret.

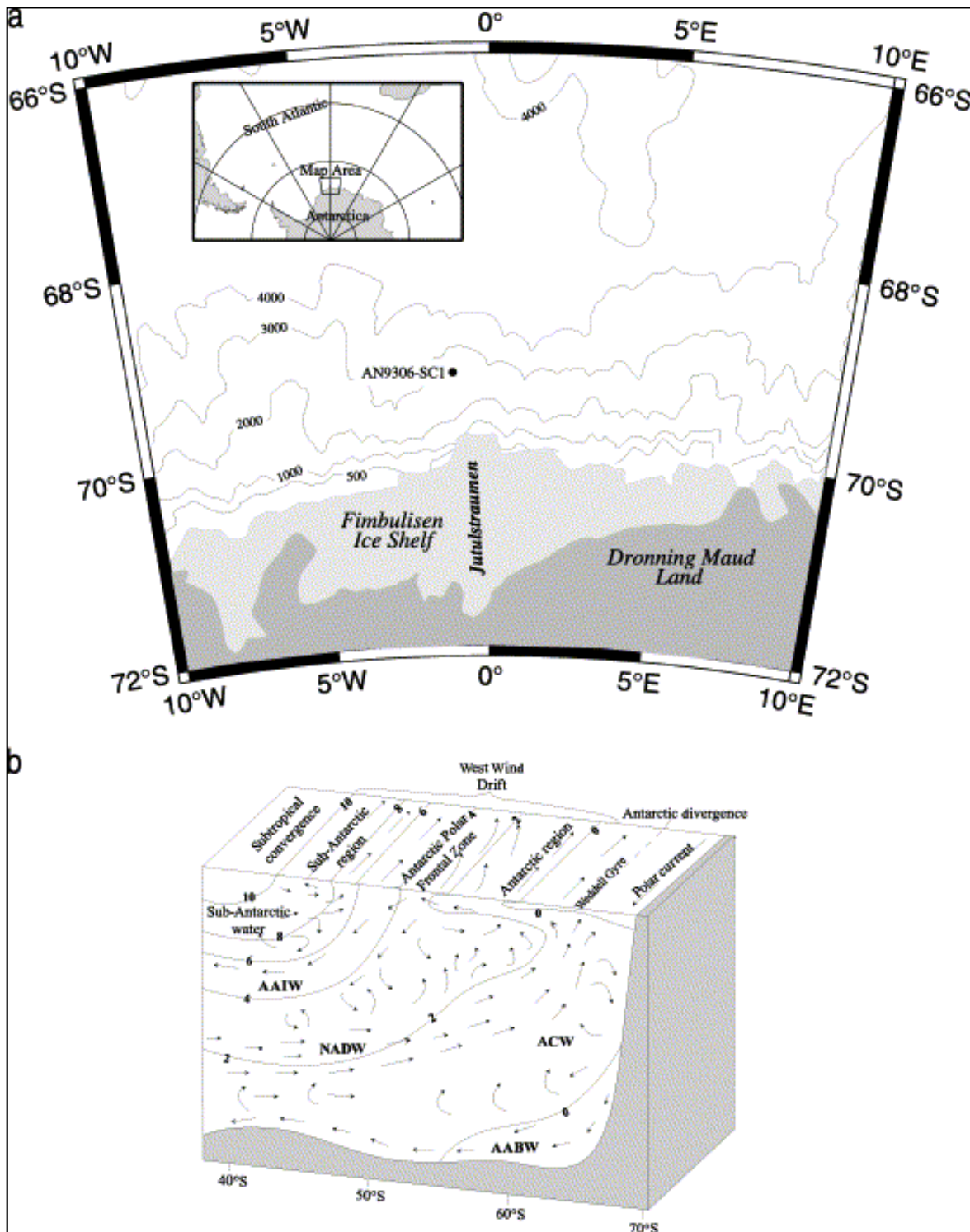


Fig. 1. (a) Location map showing the position of core AN9306-SC1 and an index map. (b) Hydrography of the Atlantic sector of the Antarctic continental margin.

[Kanfoush et al., 2000] use records of ice-rafted debris (IRD) concentrations from the last glacial cycle in cores from the South Atlantic to indicate that periods of increased iceberg production from the Antarctic Ice Sheet (AIS) coincide with periods of increased NADW flow. While the core we present from the continental margin off Dronning Maud Land does not have the same temporal resolution as the cores studied by [Kanfoush et al., 2000], it carries a continuous record that extends back to 1.3 Ma. We use this core to indicate that waters along the Antarctic continental margin have been influenced by NADW for most of this

period, and that the apparent degree of influence reflects the NADW production in the Atlantic ocean.

2. Material and methods

Cores AN9306-SC1 and AN9306-GC1 were retrieved from 2420 m water depth (position: 1°3'W, 69°13.4'S). The core site (Fig. 1a) was located on a bathymetric high in order to avoid potential problems related to down-slope mass movements and erosion. The sediments at the site are seismically well stratified on 4×40 cu in air gun and 3.5-kHz records. The Trolltunga ice tongue covered the site before this broke off during 1967, and was initially sampled to attempt to find a sedimentary record to characterise the behaviour of this glacial feature. Core AN9306-GC1 (6 m length) was retrieved using a traditional gravity corer as a test of the seafloor conditions before AN9306-SC1 (12.5 m length) was retrieved using a Selcorer®. This corer utilises the water pressure at the seafloor to hammer itself into the sediments. After retrieval the cores were cut into 1 m long sections and kept cool and upright until opening and splitting onshore. Before splitting, whole core magnetic susceptibility was determined by running the core sections through a 12.5 cm diameter circular Bartington sensor (MS2C), using an automatic transportation and recording system. This enabled correlation of the two cores. However, the gravity core was only used for preliminary amino acid age determinations before work on the Selcore was initiated. After splitting, core AN9306-SC1 was sampled continuously for palaeomagnetic analyses by pressing plastic boxes (2.2×2.2×2.0 cm) vertically into the cleaned surfaces of the split core sections. These samples, with a few additions, were also used for water contents, grain size, total carbon (TC) and total organic carbon (TOC) and stable isotope analyses.

Magnetic susceptibility was measured on the samples using a Kappabridge KLY-2 (Agico). Magnetic coercivity and thermal unblocking spectra were used to investigate the magnetic mineralogy. The direction and intensity of the natural remanent magnetisation were determined on a three-axis Cryogenic magnetometer (CCL GM400/500), located in a low-field room ($H_{\text{AMBIENT}}=200$ nT). A pilot suite of 54 samples was alternating field (AF) demagnetised in 5–10-mT steps in a mu-metal shielded two-axis tumbler to 60 mT. A spurious component was removed in most samples after 5–15 mT AF demagnetisation, above which orthogonal plots show a straight line to the origin. Medium destructive fields ranged between 10 and 60 mT. The softest magnetisations were associated with intervals carrying inferred geomagnetic excursions. All remaining samples (460) were subsequently demagnetised in 40 mT.

Approximately 20 tests of *Neogloboquadrina pachyderma* (*sin*) were picked from each of the 521 palaeomagnetic samples. Oxygen and carbon stable isotopes were measured on these in a Finnigan MAT 251 mass spectrometer at the stable isotope laboratory, University of Bergen.

Grain sizes were determined by sieving through 2-mm and 63- μ m sieves.

The IRD content was determined by examining radiographs and counting grains larger than 2 mm in every other 2-cm section of the core.

TC contents were measured in a LECO LR 12 Carbon Determinator by combustion of approx. 500 mg of bulk sediment. TOC was analysed after dissolution of the carbonate in diluted (0.1 M) hydrochloric acid, washing in distilled water and drying. Calcium carbonate content is calculated as per cent of dry bulk sediment weight, by the equation

$$\text{CaCO}_3 = (\text{TC} - \text{TOC}) \times 8.33$$

and is presented as per cent of dry bulk sediment.

¹⁴C Accelerator mass spectrometer (AMS) ages were determined at 21 and 67 cm depth (Table 1) from about 15 mg of *Neogloboquadrina pachyderma* (*sin*) tests picked from samples of between 2 and 5 cm length of core. The ¹⁴C AMS

dating itself was performed by Beta Analytic, Florida.

Table 1. Results of ^{14}C AMS dates and amino acid age estimates

Depth (cm)	Age (yr)	Error (yr)	Alle/Ile	Lab no.	Comment
21	17 800	100	NA	Beta 80857	AMS
67	34 470	480	NA	Beta 80858	AMS
54.6	45 000	10 000	0.046	BAL 3256	AA
98.6	92 000	11 000	0.083	BAL 3013	AA gravity core
103.6	95 000	9 000	0.085	BAL 3223	AA
131	158 000	21 000	0.132	BAL 3224	AA
184.7	180 000	21 000	0.148	BAL 3257	AA
203.5	202 000	23 500	0.164	BAL 3225	AA
240.3	225 000	31 500	0.183	BAL 3258	AA
312.6	320 000	32 000	0.254	BAL 3017	AA gravity core

AMS dates are indicated by 'AMS' in the comment column, whereas amino acid analyses are indicated by 'AA'. 'AA gravity core' data are from a gravity core (AN9306-GC1) taken at the same site.

Amino acid ratios **D**-alloisoleucine/**L**-isoleucine (Alle/Ile) were also determined on tests of *Neogloboquadrina pachyderma* (sin) using an automatic ion exchange amino acid analyser at the Bergen Amino Acid Laboratory. The Alle/Ile ratio is between 0.01 and 0.02 in living organisms, but approaches 1.3 at chemical equilibrium. The equilibrium is achieved through a racemisation reaction that depends on both time and temperature and on the species on which the analyses are performed. Thus the temperature must be known or assumed in order to obtain an age. Hydrographic sections (Fig. 1b) indicate that the present water temperature at the sample site is close to 0°C. Because of the importance of the colder glacial periods we have assumed an average seafloor temperature of -1.5°C (i.e. close to freezing point) for the age calculations. The amino acid ages were obtained from the Alle/Ile ratios by using the methods and reaction kinetics outlined in [Haugen and Sejrup, 1992].

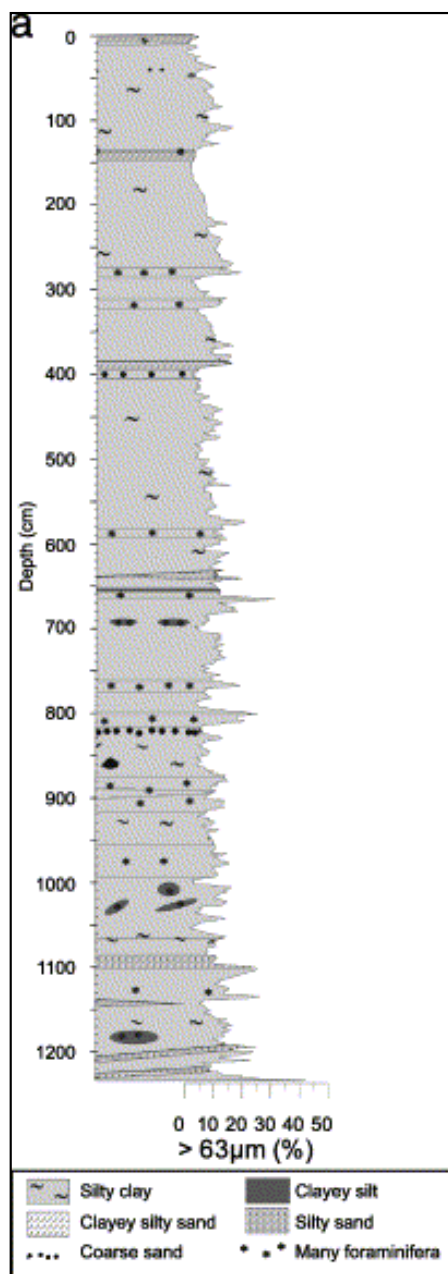
2.1. Spectral analyses

Spectral analyses and cross-correlations were performed using the SPECTRUM program ([Schulz and Stattegger, 1997]). The program was especially developed for unevenly spaced time series, and eliminates the need for interpolations to regular intervals.

3. Results

3.1. Age determination

Fig. 2a,b shows the results. A time frame for sediment accumulation is conveyed from the palaeomagnetic inclinations that define the Brunhes/Matuyama boundary (B/M) at 780 kyr (780 cm core depth). Below the Jaramillo normal polarity sub-chron (J) at 0.986 ± 0.005 Ma to 1.053 ± 0.006 Ma ([Singer et al., 1999]) (962–1032 cm core depth), a short shallow inclination interval within the Matuyama reversed chron is interpreted to represent the Cobb Mountain (CM) excursion, dated to 1.19 Ma (1122–1136 cm core depth) and with a duration of 25 kyr ([Shackleton et al., 1990]). We also believe that the fluctuation in inclination at 460 ka (460–480 cm core depth) represents the Emperor magnetic (EM) excursion and the spike at 1.105 Ma (1056 cm core depth) is the Punaruu event (PU) ([Singer et al., 1999]). Further refinement of the age model is obtained through correlation with the oxygen isotope curve from ODP Site 846 ([Mix et al., 1995]) and the deuterium results (Fig. 2b) from the Vostok ice core ([Petit et al., 1999]).



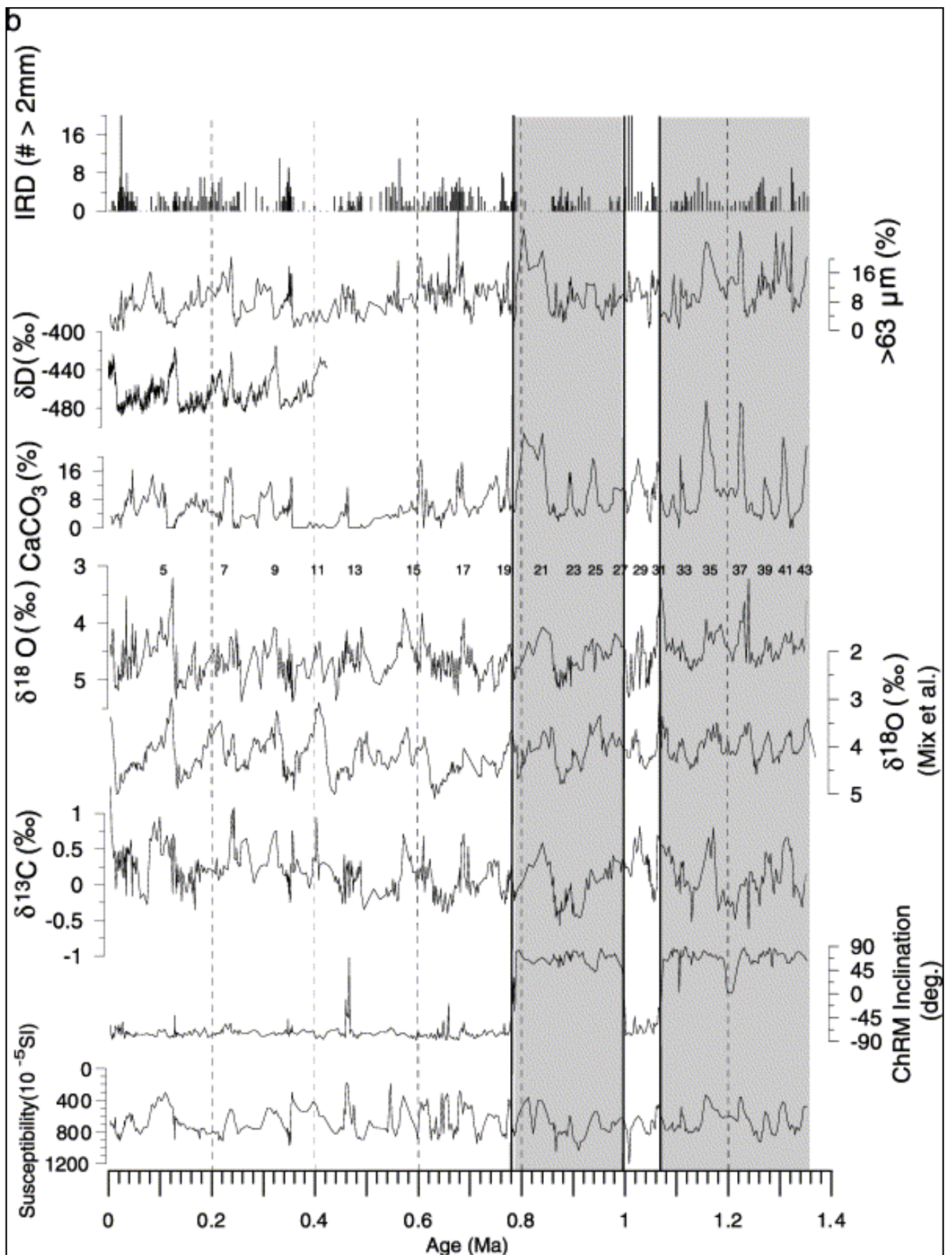


Fig. 2. (a) Lithostratigraphic column based on visual descriptions. The sand content has been used as the right-hand edge of the column. (b) The results of the analyses performed during this study. Deuterium results from the Vostok ([Petit et al., 1999]) ice core and $\delta^{18}\text{O}$ results from [Mix et al., 1995] are shown for comparison. Odd-numbered MISs are indicated above the oxygen isotope curve. The shaded regions indicate reversed magnetic polarity.

Amino acid analyses (Fig. 3) support the age model. The age model indicates that most of the Holocene is missing from the core. We believe this is because the coring procedure involved 5–10 m of free fall. Some compression of the sediment stratigraphy or refusal of the corer near the end of penetration is also likely as penetration was in excess of 15

m, whereas the recovery was 12.5 m. No gaps occur in the recovered core and the age model indicates a sedimentation rate of about 1 cm/1000 yr.

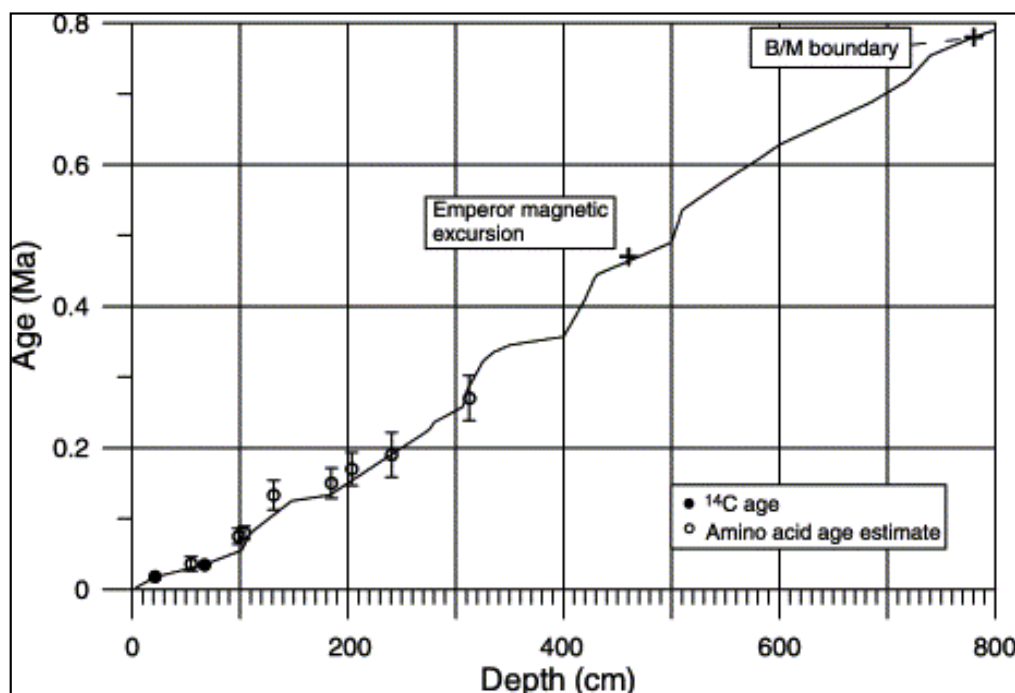


Fig. 3. Time/depth model developed for the upper 800 cm of the core. The Brunhes/Matuyama (B/M) boundary and the Emperor magnetic excursion are indicated. Filled black circles are the results of ^{14}C analyses, whereas open circles with error bars are the results of the amino acid ages.

3.2. Carbon isotopes

The $\delta^{13}\text{C}$ curve (Fig. 4) shows glacial to interglacial changes that are similar to deep sea records from the central Atlantic (e.g. ODP Site 607, [Raymo et al., 1997]). The curve varies between -0.62 and 1.09‰ whereas results from Site 607 are between -0.81 and 1.16‰ . The averages are 0.12 and 0.37‰ respectively.

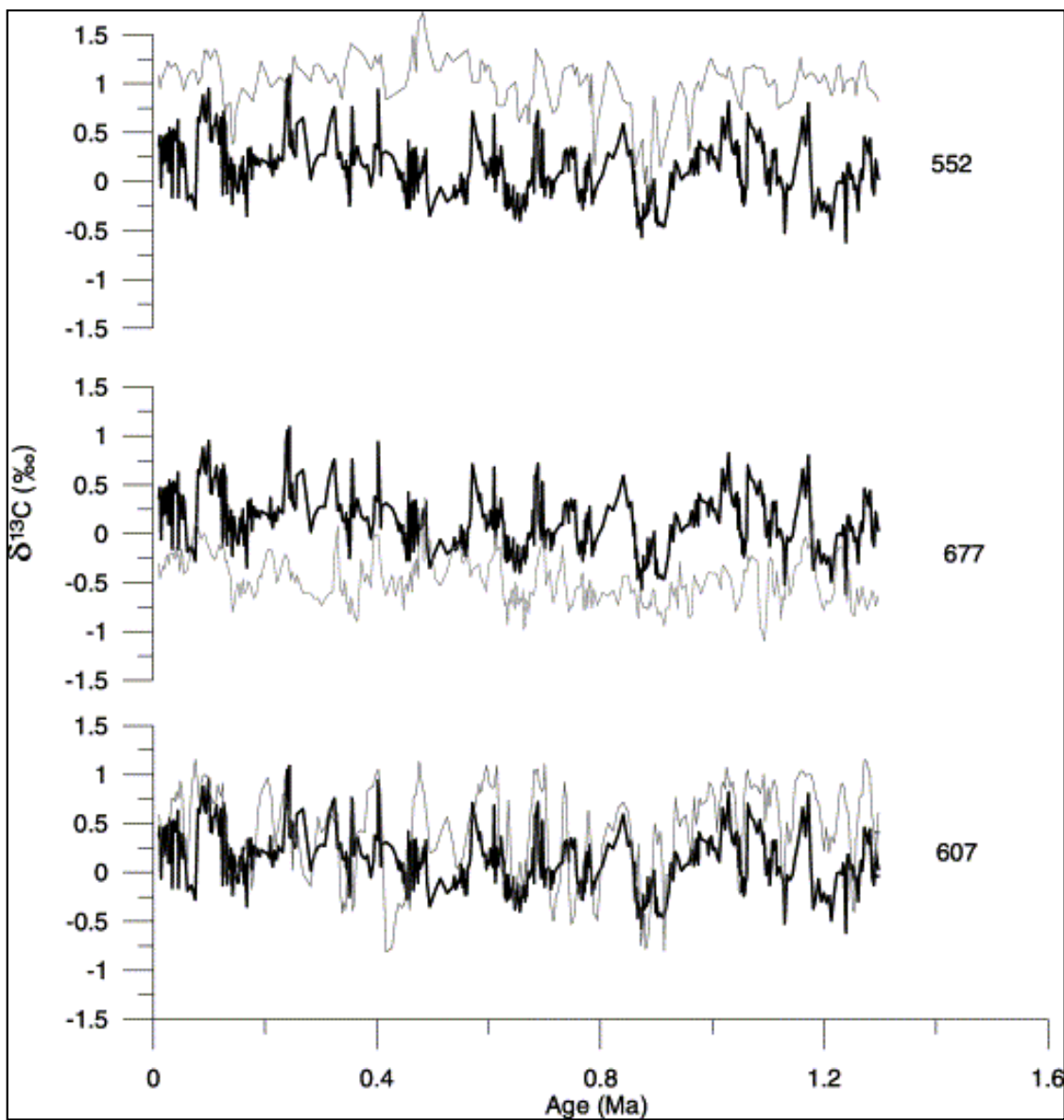


Fig. 4. $\delta^{13}\text{C}$ development compared to ODP Sites 552, 677 and 607. Site 607 is in the central Atlantic Ocean, Site 552 in the North Atlantic and Site 677 in the Pacific Ocean. Our results are the thick curves on each panel.

3.3. Carbonate and organic carbon variability

Organic carbon contents are persistently low, less than 1%, throughout the core. The inorganic carbon (carbonate) is almost exclusively the cause of variations in TC content. Visual inspection has revealed that high carbonate contents are found in intervals where there is a very high concentration of *Neoglobobulimina pachyderma* (sin), the dominating foraminiferal species in the samples. This influence also shows up in the parallelism between the carbonate curve and the content of sand-sized particles ($\% > 63 \mu\text{m}$ and includes foraminifera) (Fig. 2 and Fig. 3). From the base of the core (MIS 43) up to MIS 15, the carbonate curve has peaks that correspond to $\delta^{18}\text{O}$ minima and $\delta^{13}\text{C}$ maxima during interglacial periods (Fig. 2b). Carbonate contents are generally higher in the lower section of the core. The mid-Pleistocene transition between about 1.0 and 0.6 Ma demonstrates a change from a period with a persistent carbonate content of more than 1–2% to a record containing periods without measurable carbonate. From MIS 13 to the present interglacial, carbonate contents have been low during the interglacials, close to 0 at their terminations. The transition is accompanied by the expected change in the spectral content with an increase in the relative energy of the 100-kyr signal (Fig. 5). The carbonate curve shows a much clearer dominance of the 40-kyr cycle prior to the transition than the $\delta^{18}\text{O}$ results (Fig. 6).

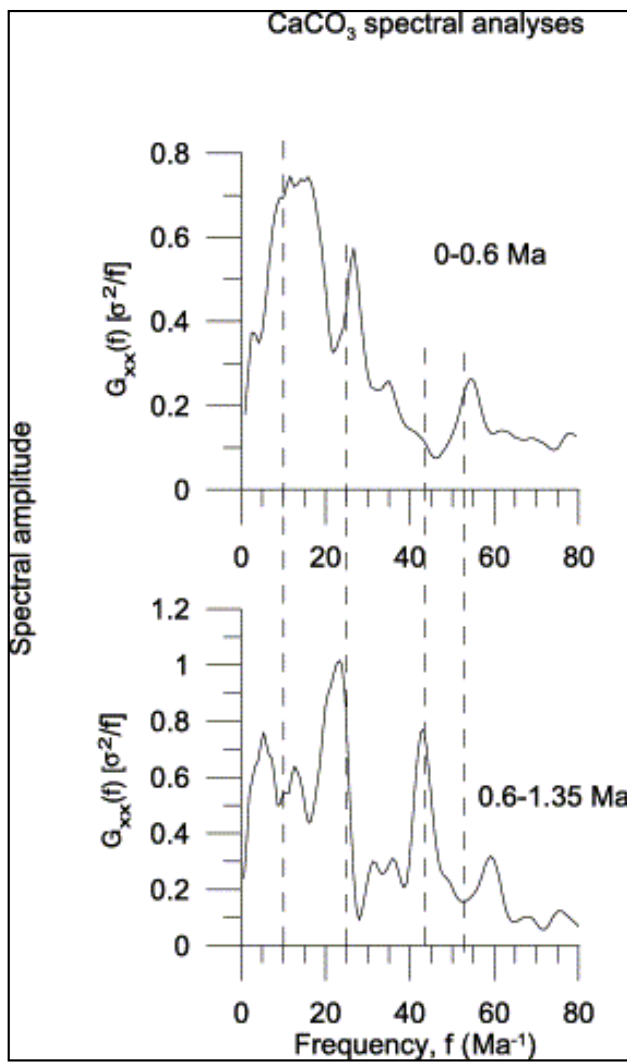


Fig. 5. Spectral analyses using SPECTRUM ([Schulz and Stattegger, 1997]) of the carbonate analyses. The change from the dominant 100-kyr periodicity (10/Ma) to the 40-kyr periodicity (25/Ma) from the upper (0–0.6 Ma) to the lower panel (0.6–1.35 Ma) is evident.

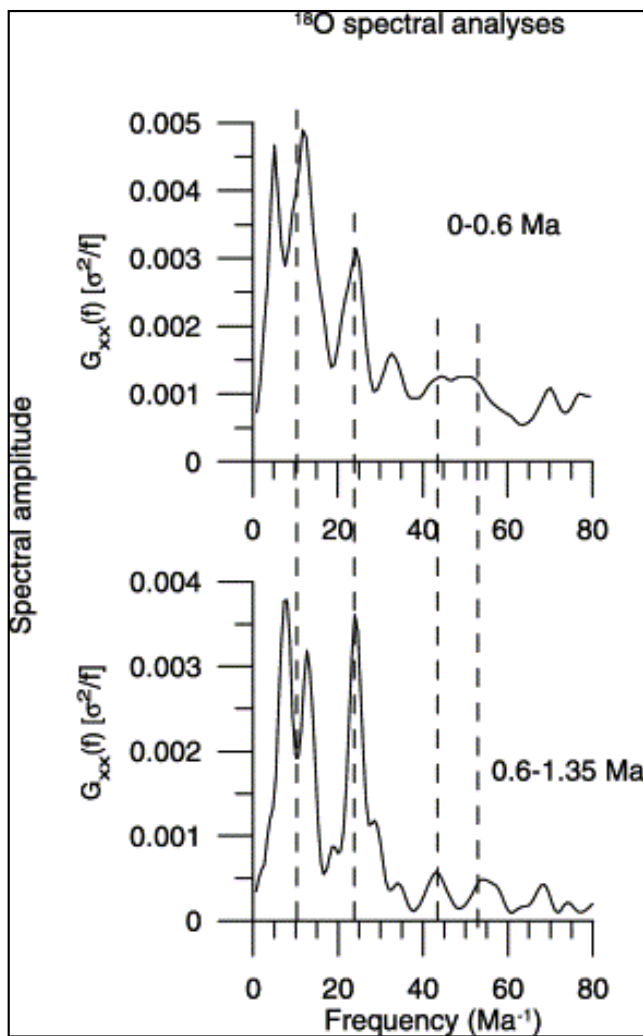


Fig. 6. Spectral analyses using SPECTRUM ([Schulz and Stattegger, 1997]) of the $\delta^{18}\text{O}$ results. The oxygen isotopes do not show as marked a difference between the dominating 100-kyr (10/Ma) and 40-kyr (25/Ma) cyclicity as do the carbonate results (Fig. 5) for the periods 0–0.6 Ma and 0.6–1.35 Ma respectively.

3.4. Magnetic susceptibility

The magnetic susceptibility is mostly attributable to the magnetite content in the finest fraction of the sediment (Fig. 7). Transport of fine sediments along Dronning Maud Land is mostly by ocean currents ([Diekmann and Kuhn, 1999]). The magnetic susceptibility is therefore a proxy of the relative importance of ocean currents on the sedimentation at the site. The magnetic susceptibilities can be seen to be lower (note reversed scale on figure) during periods with carbonate peaks. The decrease from more carbonate-poor intervals is, however, greater than can be accounted for by dilution of the magnetic minerals by carbonate alone and suggests that there is also a change in sediment provenance involved. The less productive, carbonate-poor periods have higher magnetic mineral content and may be from a greater contribution from the Proterozoic volcanic rocks and mafic intrusives on Dronning Maud Land ([Tingey, 1991]). We interpret this as an indication of the increased contribution of glacially derived sediments during the glacials.

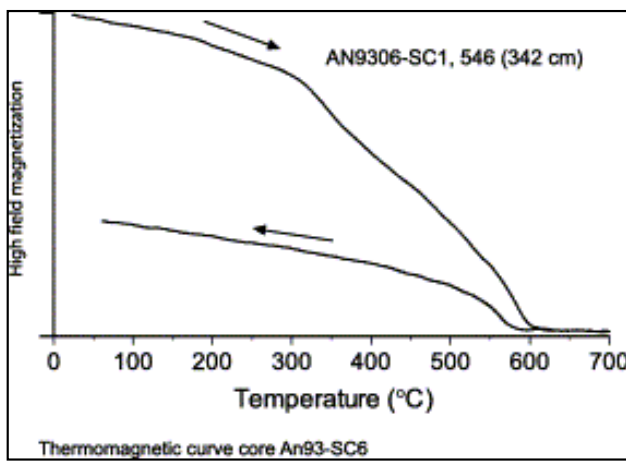


Fig. 7. Typical thermomagnetic curve of dried bulk sample (342 cm) heated in air (20°C/min) in a field of 450 mT. The heating curve exhibits a typical maghaemite inversion feature around 350°C, followed by a Curie point of around 590°C attributed to magnetite. The slightly lower Curie point defined by the cooling curve is attributed to thermal hysteresis.

3.5. Ice-rafted debris

The trends in the IRD data broadly follow the interglacial–glacial cycles, with interglacial periods having a somewhat higher concentration than the glacial periods for the last 400 kyr. However, the trend for the part of the core older than 1 Myr shows the opposite trend, with glacial periods associated with more IRD. During MIS 11 there was an extended period with very little IRD. The IRD-poor interval around 0.8 Ma corresponds to an interval with very high carbonate contents and may therefore be due to dilution by a high rate of biogenic sedimentation.

4. Discussion

[Matsumoto et al., 2001] use $\delta^{18}\text{O}$ analyses of foraminifera to show that the present upwelling of Circumpolar Deep Water and NADW south of the APF (Fig. 1) and along the Antarctic continental margin also occurred during the last glacial maximum. They argue that this is because the position of the APF is governed by bathymetry and continental configurations combined with predominantly westerly, circumpolar winds. We explore this further back in time by examining the influence of NADW at our core site. The present upwelling means that the surface waters along the Antarctic continental margin are influenced by similar water masses to those at depth below the APF (Fig. 1). Similarities in the development observed in our core and from the neighbourhood of the APF will therefore indicate a persistent influence from NADW.

Our core contains carbonate-depleted intervals that we, as do [Grobe and Mackensen, 1992], interpret to be a response to dissolution rather than non-deposition. [Hodell et al., 2001] interpret similar dissolution events at ODP Site 1089, near the APF, to be the result of adjustments of the lysocline. These dissolution events occur at the transition between interglacials and glacials in a manner similar to results obtained from cores from the Pacific and Indian oceans. At Site 1089 the $\delta^{18}\text{O}$ signal leads the carbonate signal by 7.6 kyr ([Hodell et al., 2001]) and occurs during periods of most rapid changes in $\delta^{18}\text{O}$, i.e. the ocean volume. Our results show a similar relationship (Fig. 8) and we interpret this as indicating that the adjustment of the lysocline proposed by [Hodell et al., 2001] also influenced the Antarctic continental margin and that NADW was an important factor in Antarctic oceanography for this period. The [Hodell et al., 2001] data go back 600 kyr. The part of our core that is older than this (Fig. 2) shows neither dissolution events nor a time lag between the oxygen isotope and the carbonate curves (Fig. 9). [Raymo et al., 1997] used $\delta^{13}\text{C}$ records from the Atlantic and Pacific oceans to map the strength of the NADW flow and its influence during the past 1.3 Myr. We adopt their method to further explore the influence of NADW back in time. We use analyses from the planktonic species *Neogloboquadrina pachyderma (sin)*, which live in the upper water masses, that we infer to be sensitive to changes in the intensity of upwelling along the continental margin.

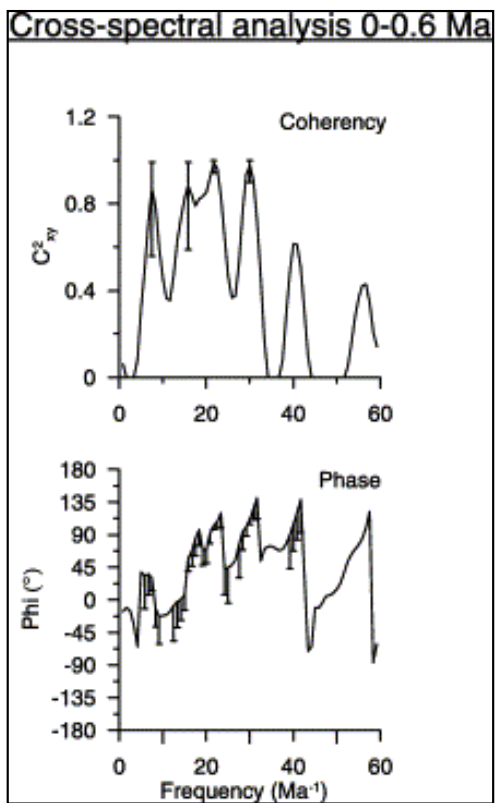


Fig. 8. Cross-spectral analyses between the carbonate analyses and the $\delta^{18}\text{O}$ results for the period 0–0.6 Ma. The phase angle for the ~100-kyr (at ~9/Ma) peak is 45° , indicating that the $\delta^{18}\text{O}$ signal leads the carbonate signal by ~12.5 kyr. Similar values are obtained for the other peaks (peak period \times phase angle/360).

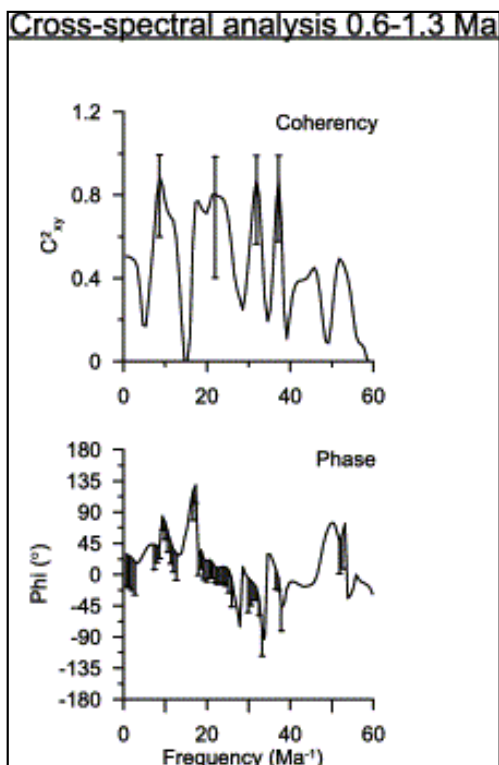


Fig. 9. Cross-spectral analyses between the carbonate analyses and the $\delta^{18}\text{O}$ results for the period 0.6–1.35 Ma. The phase angle is about 0 for the dominating 40-kyr (25/Ma) climatic cycle.

The similarity of our $\delta^{13}\text{C}$ results to those of ODP Site 607 in the Atlantic Ocean indicates that the upwelling of NADW plays an important role in controlling the isotopic composition found in our core. In general, our values are somewhat lower than those from Site 607, in agreement with a somewhat longer transportation path of NADW to the Antarctic continental margin. The isotopic records may, however, also be due to changes in the overall isotopic composition of the

oceans. To explore this further we found, in a similar manner to [Raymo et al., 1997], the relative strength of the NADW influence by calculating an index given by:

$$\text{NADW}_{\text{index}} = \frac{\text{SC6} - 677}{552 - 677}$$

where SC6 are our $\delta^{13}\text{C}$ results, and 552 and 677 those from ODP Sites 552 in the North Atlantic and 677 ([Shackleton et al., 1990]) in the Equatorial Pacific respectively. The values used for 552 and 677 are those found by interpolating to the same age as that of the SC6 data. As can be anticipated from the isotope curves, both our data (Fig. 10) and those from 607 ([Ruddiman et al., 1989]) show similar index trends, with 607 having the greatest NADW index. Both data sets show the lowest index values between about 400 kyr BP and 600 kyr BP, where they approach Pacific values. This precedes the period when the most extensive carbonate dissolution occurs, during MIS 13 and 11, and the final stage of the transition to the 100-kyr climatic cyclicity. [Raymo et al., 1997] show that the $\delta^{13}\text{C}$ gradient between the Atlantic and Pacific oceans remains at about the same level for the whole study period and that the $\text{NADW}_{\text{index}}$ therefore is probably a reflection of NADW influence. We thus conclude that NADW has been an important contributor to Antarctic continental margin hydrography also from 600 ka to 1.35 Ma BP, and therefore during the whole period covered by our core.

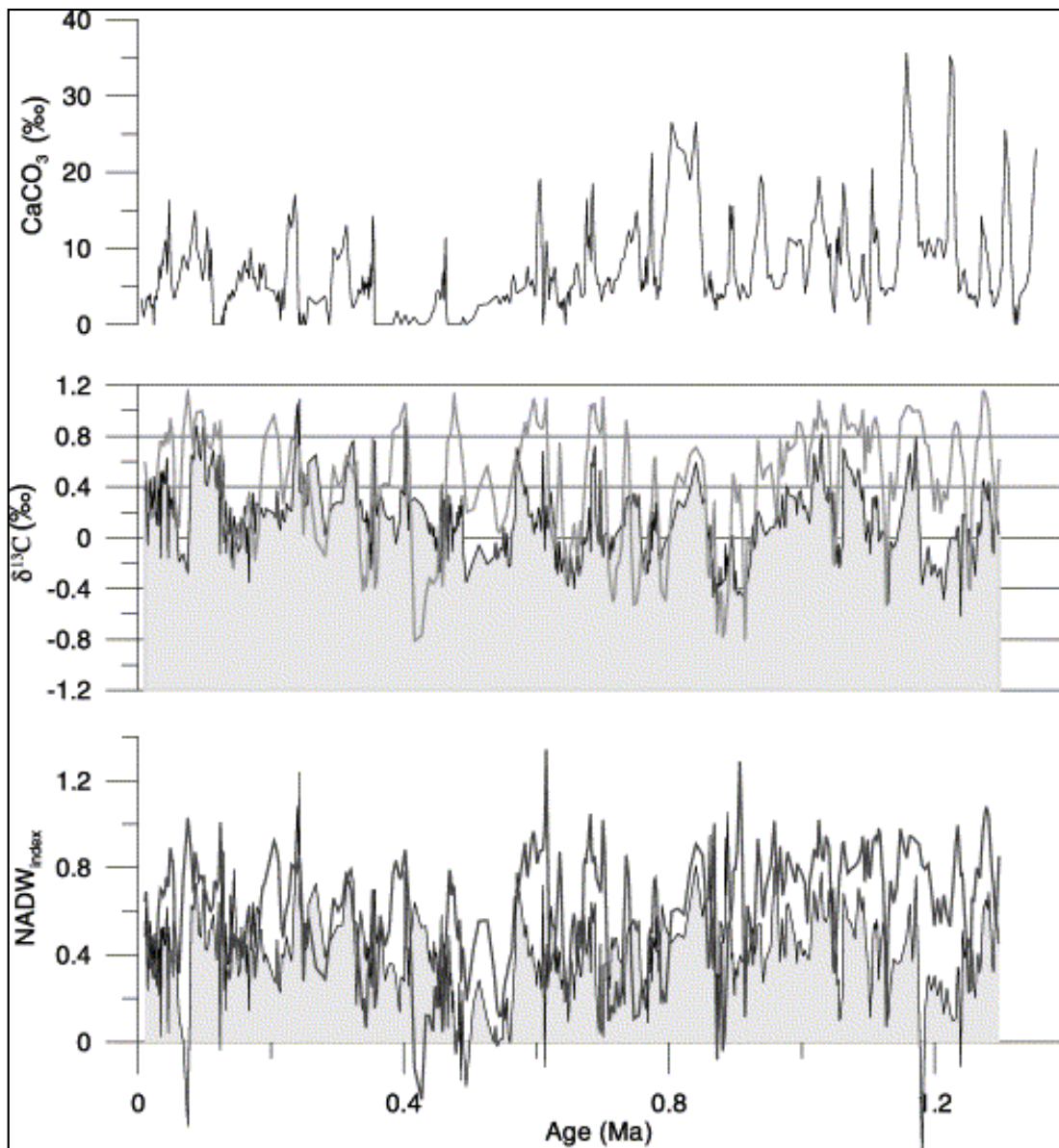


Fig. 10. (Lower panel) The $\text{NADW}_{\text{index}}$ (see text) calculated for our core (AN9306-SC1) and ODP site 607. Our results are shaded. (Middle panel) The results of $\delta^{13}\text{C}$ analyses of the same two cores. (Top panel) Carbonate content through our core for comparison with the lower panels.

The persistent carbonate content during this oldest part of the core means that, in the absence of changes in sedimentation rate, the carbonate signal can be interpreted as an indication of a biogenic production that was greatest during warm periods (up to 30% CaCO_3), but that was also significant ($>4\%$) during glacial periods identified by high $\delta^{18}\text{O}$ values. Sea ice has an important role in limiting primary production in the Southern Ocean ([[Bonn et al., 1998](#)]). The carbonate contents may therefore indicate that there were significant areas of ice-free surface waters, at least during the summers, during most of this early period, even during the glacials.

The IRD signal changes character at the mid-Pleistocene transition and indicates that the AIS may have changed its response to climatic forcing during this period. Prior to the transition, cold periods correspond to periods with higher IRD levels whereas after 400 ka, there is a trend indicating more IRD during the interglacials. [ÓCofaigh et al. \(2001\)](#) indicate that this latter trend is the result of reduced sedimentation rates during the interglacials. [Fig. 3](#) shows that there was a high sedimentation rate during MIS 11 and 13 that can explain the lack of IRD. However, the shorter climatic cyclicity and the temporal resolution of our age model means that we are unable to differentiate between sedimentation rates during cold and warm periods for the older part of the core. One speculation is that there was, prior to the mid-Pleistocene transition, a dilution during interglacials that was due to an increased supply of meltwater-derived sediments.

MIS 11 has been proposed to have been oceanographically anomalous ([[Raymo et al., 1997](#) and [Hall et al., 2001](#)]) or exceptionally long. Our data indicate an oceanographic situation characterised by an especially low $\text{NADW}_{\text{index}}$ that appears to end in conjunction with the carbonate dissolution events during MIS 11 and 13.

Whether the extended dissolution is truly a demonstration of a global oceanographic anomaly at the end of the mid-Pleistocene transition or not, cannot be clarified from our data, but the phenomenon does appear to be characteristic of the Atlantic sector of the Southern Ocean as [[Mackensen et al., 1989](#)] presented similar results for this period.

5. Conclusions

The investigated core shows a complete record from about 8 ka to 1.35 Ma. The influence from NADW, as seen from the $\text{NADW}_{\text{index}}$ ([[Raymo et al., 1997](#)]), parallels the index values in the central Atlantic Ocean and shows that the continental shelf off Dronning Maud Land appears to have been influenced by upwelling of NADW for the whole of this period.

The influence from NADW was at its lowest during the mid-Pleistocene transition.

Temporally extended and/or intense carbonate dissolution during MIS 11 and 13 followed this period with low $\text{NADW}_{\text{index}}$ values. Both these and shorter or less intense periods of carbonate dissolution, which occurred during the interglacial to glacial transitions after MIS 11, are interpreted to be due to a shallowing of the lysocline. The similarity to the dissolution events reported from ODP Site 1089, near the APF ([[Hodell et al., 2001](#)]), demonstrates the oceanographic connection implied by the upwelling of NADW.

The persistent carbonate contents in the sediments older than the mid-Pleistocene transition indicate that there was significant primary production and therefore open water even during the coldest (glacial) conditions at this time.

The IRD concentration after the mid-Pleistocene transition is somewhat higher during interglacials whereas the opposite is true prior to it. A speculation is that this is because sedimentation rates were low during interglacials after the transition, whereas they may have been somewhat higher due to a component of meltwater-derived sediments before it.

Acknowledgements

We would like to thank the captain and crew of M/S *Lance* for all their help in retrieving the cores used in this study. We would also like to thank D.A. Warnke and A. Negri for their very helpful reviews.

References

- Bonn et al., 1998. W.J. Bonn, F.X. Gingele, H. Grobe, A. Mackensen and D.K. Futterer, Palaeoproductivity at the Antarctic continental margin: opal and barium records for the last 400 ka. *Palaeogeogr. Palaeoclimatol. Palaeoecol.* **139** (1998), pp. 195–211.
- Broecker, 1998. W.S. Broecker, Paleocean circulation during the last deglaciation: A bipolar seesaw?. *Paleoceanography* **13** (1998), pp. 119–121.
- Diekmann and Kuhn, 1999. B. Diekmann and G. Kuhn, Provenance and dispersal of glacial-marine surface sediments in the Weddell Sea and adjoining areas, Antarctica: ice-rafting versus current transport. *Mar. Geol.* **158** (1999), pp. 209–231.
- Grobe and Mackensen, 1992. H. Grobe and A. Mackensen, Late Quaternary climatic cycles as recorded in sediments from the Antarctic continental margin. The Antarctic paleoenvironment: A perspective on global change. *AGU Antarct. Res. Ser.* **56** (1992), pp. 349–376.
- Hall et al., 2001. I.R. Hall, I.N. McCave, N.J. Shackleton, G.P. Weedon and S.E. Harris, Intensified deep Pacific inflow and ventilation in Pleistocene glacial times. *Nature* **412** (2001), pp. 809–812.
- Haugen and Sejrup, 1992. J.E. Haugen and H.P. Sejrup, isoleucine epimerization kinetics in the shell of *arctica-islandica*. *Norsk Geol. Tidsskr.* **72** (1992), pp. 171–180.
- Hodell et al., 2001. D.A. Hodell, C.D. Charles and F.J. Sierro, Late Pleistocene evolution of the ocean's carbonate system. *Earth Planet. Sci. Lett.* **192** (2001), pp. 109–124.
- Kanfoush et al., 2000. S.L. Kanfoush, D.A. Hodell, C.D. Charles, T.P. Gullerson, P.G. Mortyn and U.S. Ninnemann, Millennial-scale instability of the Antarctic Ice Sheet during the last glaciation. *Science* **288** (2000), pp. 1815–1818.
- Mackensen et al., 1989. A. Mackensen, H. Grobe, H.W. Hubberten, V. Spiess and D.K. Futterer, Stable isotope stratigraphy from the Antarctic Continental Margin during the last one million years. *Mar. Geol.* **87** (1989), pp. 315–321.
- Matsumoto et al., 2001. K. Matsumoto, J. Lynch-Stieglitz and R.F. Anderson, Similar glacial and Holocene Southern Ocean hydrography. *Paleoceanography* **16** (2001), pp. 1–10.
- Mix et al., 1995. Mix, A.C., Le, J., Shackleton, N.J., 1995. Benthic foraminiferal stable isotope stratigraphy of Site 846: 0–1.8 Ma. In: Pisias, N.G., Mayer, L.A., Janecek, T.R., Palmer-Julson, A., van Andel, T.H. (Eds.), Proc. ODP Sci. Results 138, 839–854.

- ÓCofaigh, C., Dowdeswell, J.A. and Pudsey, C.J., 2001. Late Quaternary iceberg rafting along the Antarctic Peninsula continental rise and in the Weddell and Scotia Seas. *Quat. Res.* **56**, pp. 308–321.
- Oppo et al., 1995. D.W. Oppo, M.E. Raymo, G.P. Lohmann, A.C. Mix, J.D. Wright and W.L. Prell, A $\delta^{13}\text{C}$ record of upper North Atlantic deep-water during the past 2.6-million years. *Paleoceanography* **10** (1995), pp. 373–394.
- Petit et al., 1999. J.R. Petit, J. Jouzel, D. Raynaud, N.I. Barkov, J.-M. Barnola, I. Basile, M. Bender, J. Chappellaz, M. Davis, G. Delaygue, M. Delmotte, V.M. Kotlyakov, M. Legrand, V.Y. Lipenkov, C. Lorius, L. Pépin, C. Ritz, E. Saltzman and M. Stievenard, Climate and atmospheric history of the past 420,000 years from the Vostok ice core, Antarctica. *Nature* **399** (1999), pp. 429–436.
- Pudsey, 1992. C.J. Pudsey, Late Quaternary changes in Antarctic Bottom Water velocity inferred from sediment grain-size in the northern Weddell Sea. *Mar. Geol.* **107** (1992), pp. 9–33.
- Raymo et al., 1997. M.E. Raymo, D.W. Oppo and W. Curry, The mid-Pleistocene climate transition: A deep sea carbon isotopic perspective. *Paleoceanography* **12** (1997), pp. 546–559.
- Ruddiman et al., 1989. W.F. Ruddiman, M.E. Raymo, D.G. Martinson, B.M. Clement and J. Backman, Pleistocene evolution of northern hemisphere climate. *Paleoceanography* **4** (1989), pp. 353–412.
- Schulz and Stattegger, 1997. M. Schulz and K. Stattegger, Spectrum: Spectral analysis of unevenly spaced palaeoclimate time series. *Comput. Geosci.* **23** (1997), pp. 929–945.
- Shackleton et al., 1990. N.J. Shackleton, A. Berger and W.R. Peltier, An alternative astronomical calibration of the lower Pleistocene timescale based on ODP Site 677. *Trans. R. Soc. Edinburgh Earth Sci.* **81** (1990), pp. 251–261.
- Singer et al., 1999. B.S. Singer, K.A. Hoffman, A. Chauvin, R.S. Coe and M.S. Pringle, Dating transitionally magnetized lavas of the late Matuyama Chron: Toward a new Ar-40/Ar-39 timescale of reversals and events. *J. Geophys. Res. Solid Earth* **104** (1999), pp. 679–693.
- Tingey, 1991. R.J. Tingey, Commentary on schematic geological map of Antarctica Scale 1:10000000. *Bur. Min. Resour. Geol. Geophys. Bull.* **238** (1991), pp. 1–30.